Multicolor tunability and upconversion enhancement of fluoride nanoparticles by oxygen dopant

Niu, Wenbin; Wu, Suli; Zhang, Shufen; Su, Liap Tat; Tok, Alfred Iing Yoong

2013

Niu, W., Wu, S., Zhang, S., Su, L. T., & Tok, A. l. Y. (2013). Multicolor tunability and upconversion enhancement of fluoride nanoparticles by oxygen dopant. Nanoscale, 5(17), 8164-8171.

https://hdl.handle.net/10356/96005

https://doi.org/10.1039/C3NR01612A

Journal Name

Dynamic Article Links ►

Cite this: DOI: 10.1039/c0xx00000x

www.rsc.org/xxxxxx

ARTICLE TYPE

Multicolor tunability and upconversion enhancement of fluoride nanoparticles by oxygen dopant

Wenbin Niu,[a] Suli Wu,[a] Shufen Zhang,*[a] Liap Tat Su[b] and Alfred Iing Yoong Tok[b]

Received (in XXX, XXX) Xth XXXXXXXXX 20XX, Accepted Xth XXXXXXXXX 20XX

DOI: 10.1039/b000000x

The ability of manipulating upconversion luminescence of lanthanide-ion doped fluoride upconversion nanoparticles (UCNPs) is particularly important and highly required due to their widely applications in color displays, multiplexing bioassays and multicolor imaging. Here, we developed a strategy for simultaneously tuning color output and enhancing upconversion emission of Yb/Er doped fluoride UCNPs, based on adjusting oxygen doping level. The synthesis of multicolored multifunctional $NaGdF_4$:Yb, Er UCNPs was used as the model host system to demonstrate this protocol. Ammonium nitrate (NH_4NO_3) was used as oxygen source and added into reaction system at the beginning stage of nucleation and growth process of fluoride UCNPs, which facilitates the formation of enough oxygen atoms and the diffusion of those into fluoride host matrix. The results revealed the multicolour output and upconversion enhancement mainly resulted from the variation of phonon energy and crystal field symmetry of host lattice, respectively. This strategy can be further expanded to other fluorides host matrices. As an example of the application, multicolored UCNPs were used as color converter in light emitting diodes, which can effectively convert near-infrared light into visible ones. It is expected these multicolored UCNPs are promising for applications in multiplexing biodetection, bioimaging (optical and magnetic resonance imaging) and other optical technologies, and the present method for the control of O^{2-} doping may also be used in other functional nanomaterials.

Introduction

The ability of tuning multicolor emission of upconversion nanomaterials is important for their myriad applications in sensing, display, light emitting technology, *in vitro* and *in vivo* bio-imaging and medical sciences.[1] As compared to the conventional organic fluorescent dyes and quantum dots, lanthanide-ion doped fluoride upconversion nanoparticles (UCNPs) show great potential technological applications,[2,3] because they exhibit low cytotoxicity,[4] high resistance to photo-bleaching and -blinking,[5] large anti-Stokes shifts,[6] narrow-band emissions, high chemical stability,[5b,7] deep penetration to biological tissues,[4b,8] and high signal-to-noise ratio. [2,9-11]

Recently, several attempts have been made to tune multicolor upconversion emission. The typical approach is doping multi-activators and adjusting their concentration in upconversion nanomaterials.[12-14] Because lanthanide ion exhibit characteristic emission bands with specific wavelengths, the multicolor output of UCNPs can be obtained by adjusting the intensities of different emission peaks of various activators through controlling their doping level in nanoparticles. However, the presence of high concentration dopant and multi-activators could result in high cross-relaxation, and thus reduce upconversion intensity.[12] Researchers have been attempting to minimize this deleterious cross-relaxation in multiply activators recently.[11] Alternatively, multicolor tuning from single lanthanide-ion activator can also greatly enrich the colors of UCNPs by controlling the relative intensities of different emission peaks.[10a,13,14] Although we had reported the manipulation of color emissions from single lanthanide-ion activator,[10,13a] the upconversion emission intensity was still sacrificed, which may limit applications of fluoride UCNPs due to the reduced emission intensity. Therefore, to ensure the application performance of UCNPs, it is important and highly required to develop a method for simultaneously tuning color output and enhancing upconversion emission, however, it is still a substantial challenge.[3e]

Here, we report a strategy for simultaneously tuning color output and enhancing upconversion emission of single lanthanide-ion activator in fluoride UCNPs, based on adjusting oxygen doping level. Er/Yb doped $NaGdF_4$ UCNPs were chosen as the model host system to demonstrate this protocol because of its multifunctional properties.[15,16] Ammonium nitrate (NH_4NO_3) was used as the oxygen source to introduce the oxygen dopant (O^{2-}) into host matrix of fluoride UCNPs. The existence of oxygen dopant in fluoride host lattice enhances phonon energy of fluoride host lattice and increases the transition probability of Er^{3+} ions, resulting in the variation of Er/Yb doped fluoride emissions from green to red. Moreover, O^{2-} ions doping also induces the great enhancement of upconversion luminescence and the splitting of red-emitting level of Er^{3+} ions due to the decrease of crystal field symmetry. In the proof-of-concept, the O^{2-} ions

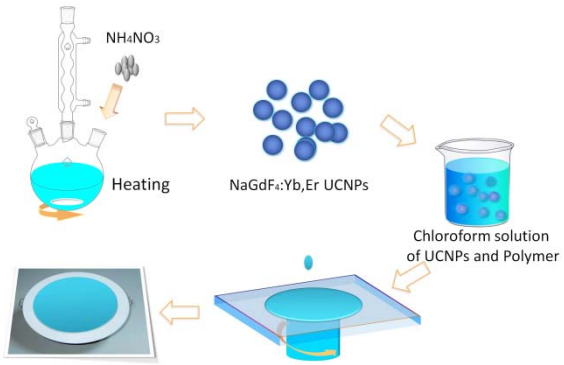

Scheme 1 Schematic illustration of preparation of multicolored fluoride UCNPs and LED devices.

doped upconversion nanoparticles were incorporated into polymer and employed as color converter in light emitting diodes (LEDs) (Scheme 1).

Experimental

Synthesis of multicolor nanoparticles

For a typical synthesis of $NaGdF_4$:Yb, Er UCNPs, a mixture of Er_2O_3 (0.02 mmol), Yb_2O_3 (0.20 mmol), Y_2O_3 (0.78 mmol) and Na_2CO_3 (1.0 mmol) was dissolved in 10 mL of 50 % aqueous trifluoroacetic acid at 80 ^oC. The residual water and acid were slowly evaporated to dryness. Then, octadecylamine (100 mmol) were added. The reaction solution was heated to 120 ^oC and maintained for 30 min under reduced pressure with magnetic stirring to remove residual water and oxygen, during which time the flask was purged periodically with dry nitrogen. The resulting optically transparent solution was heated to 300 ^oC and maintained for 1 h under a nitrogen atmosphere. During the heating process, a certain amount of NH_4NO_3 was added into the reaction solution when the temperature rose to 250 ^oC. After heating was stopped, the reaction solution was cooled to 70 ^oC, and absolute ethanol was added to precipitate the fluorides UCNPs. The products were isolated by centrifugation. This procedure was repeated at least two times. The resulting nanoparticles were dried under vacuum for 24 h.

$NaGdF_4$:Yb, Er UCNPs with multicolor output were obtained by changing the added amount of NH_4NO_3 while other conditions were held constant. The procedure for the synthesis of $NaYF_4$:Yb, Er and $NaLuF_4$:Yb, Er UCNPs was similar to the above description.

Synthesis of methyl methacrylate-butyl acrylate copolymer (P(MMA-co-BA))

1.0 g of AIBN was added into the flask containing 150 mL of petroleum ether. The solution was heated to 80 ^oC. Then a mixture solution of methyl methacrylate (15 g) and butyl acrylate (15 g) was dropped into the above solution. The polymerization proceeded for 6 h at 80 ^oC. The resulting turbid solution was cooled to room temperature. The P(MMA-*co*-BA) was obtained by precipitation and dried under vacuum for 24 h.

Preparation of nanocomposite and coating on NIR-LED devices

Various amounts of $NaGdF_4$:Yb, Er UCNPs with multicolor output (100 mg for 50 wt %, 70 mg for 35 wt %, 40 mg for 20 wt %) were dispersed in 3 mL of chloroform solution. Then 100 mg of P(MMA-*co*-BA) was added and the mixture was sonicated for 10 min. The chloroform was then slowly evaporated, and the polymer thin film was coated on the lens of LEDs by solvent casting.

Characterization

Upconversion fluorescence spectra were measured on a Hitachi F-4500 fluorescence spectrophotometer under the excitation of a 980 nm diode laser. The transmission electron microscopy (TEM) images were taken with a Tecnai F20 S-TWIN microscope transmission electron microscope operating at 200 kV. Powder X-ray diffraction patterns were recorded on a Rigaku D/MAX-2400 diffractmeter with Cu-Ka radiation. The scanning-step size was 0.02^o 2θ. X-ray fluorescent spectra were measured with a XRF-1800 spectrophotometer of SHIMADZU. Raman spectra were collected on a DL-2 Raman spectroscopy equipped with a 244 nm laser (Dalian Institute of Chemical Physics, China).

Results and discussion

Preparation and structure characterization of $NaGdF_4$:Yb, Er UCNPs

To introduce the oxygen dopant into host matrix of fluoride UCNPs, ammonium nitrate (NH_4NO_3) was used as the oxygen source and added into reaction system at 250 ^oC, because which facilitate the formation of enough oxygen and the diffusion of formed oxygen dopant into host matrix (Fig. S1 and S2).[17] The O^{2-} doping level in fluoride UCNPs was controlled by adjusting

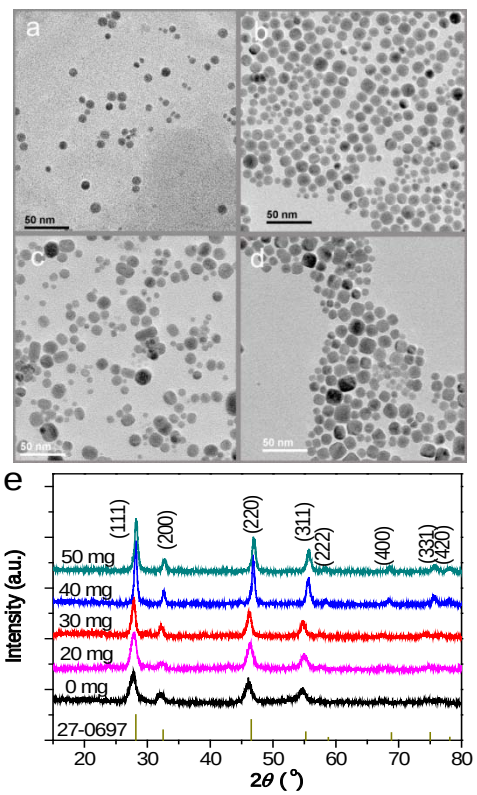

Fig. 1 TEM images of $NaGdF_4$:Yb, Er UCNPs (2mmol) prepared with various amounts of NH_4NO_3, 300 ^oC, 1h, (a,0 mg; b, 20 mg; c, 30 mg; d, 40 mg) and XRD patterns (e) of the corresponding samples.

the amount of NH_4NO_3. TEM in Fig. 1 shows $NaGdF_4$:Yb, Er UCNPs prepared with varying amounts of NH_4NO_3 are all near-spherical shape. The mean size of nanoparticles increases from 7 nm, to 10, 13 and 14 nm with the amount of NH_4NO_3 increased from 0 mg, to 20, 30 and 40 mg, respectively. This is because the formed oxygen increased the concentration of anion in reaction solution and promoted the growth of $NaGdF_4$:Yb, Er UCNPs, and thus resulted in the increase of nanoparticles size. This is in agreement to X-ray diffraction patterns (XRD) of UCNPs where the diffraction peak width narrowed with the increase of NH_4NO_3.[16b] XRD pattern of those particles shows that there are cubic α-$NaGdF_4$:Yb, Er (JCPDS No.27-0697) and there were no GdOF and no other phase and impurities were formed.[18] X-ray fluorescent spectroscopy (XRF) was used for the measurement of doped oxygen content in $NaGdF_4$ UCNPs. It is shown that the oxygen content in $NaGdF_4$:Yb, Er UCNPs increased gradually from 2.09 wt% to 10.10 wt% with the increase of the amounts of NH_4NO_3 from 20 mg to 50 mg (**Table 1**). This result was further validated by XRD pattern where the diffraction peak positions shifted to the high-angle direction (*e.g.* (200), (220) and (311), Fig. S3), indicating that the lattice cell contracted as O^{2-} partially substituted for fluorine ions (F^-). It is noted that the lattice cell contracted though the radius of O^{2-} (140 pm) was larger than that of F^- (133 pm), because one O^{2-} can substitute two F^- positions in host lattice due to the electrical neutrality of whole fluoride particle,[19] which further implied the incorporation of oxygen into $NaGdF_4$ host.

Table 1 XRF results of O^{2-} dopant content in $NaGdF_4$:Yb, Er particles prepared with various amounts of NH_4NO_3.

Amounts of NH_4NO_3 (mg) [a]	20	30	40	50
Oxygen content(wt%)	2.09	4.56	7.13	10.10

[a] Added amount of NH_4NO_3 per 2 mmol $NaGdF_4$:Yb, Er.

Multicolor tunability and enhancement of upconversion emission

Fig. 2a shows $NaGdF_4$:Yb,Er UCNPs prepared with no oxygen doping show the strong green emission peaks around 520 and 540 nm, which can be assigned to the $^2H_{11/2}$, $^4S_{3/2}\rightarrow{}^4I_{15/2}$ transitions, and the relative weak red emission peaks of $^4F_{9/2}\rightarrow{}^4I_{15/2}$ transition of Er^{3+} ion.[20,21] The doping of O^{2-} ions in UCNPs led to a fast increase in red emission of Er^{3+} ions, resulting that the intensities ratio of green to red emissions gradually decreases from 2.60 to 0.02 (Fig. S4), and therefore the color output of $NaGdF_4$:Yb,Er could be finely tuned from green to red. When the added amount of NH_4NO_3 was increased to 40 mg, the red emission increased significantly and pure red emission was observed (Fig. 2b and S4). To investigate the multicolor output mechanism, we further tested the upconversion mechanism of $NaGdF_4$:Yb,Er UCNPs. The number of photons involved in the upconversion process was calculated by the power dependent luminescence intensities in log-log plots. The experimental data for 550 and 650 nm emission bands of $NaGdF_4$:Yb, Er were fitted with a straight line with a slope of ~2 (Fig. 2c and S5), indicating a two-photon emission process.[10a,14b] According to the two-photon involved energy transfer upconversion process (Fig. 2d), the nonradiative

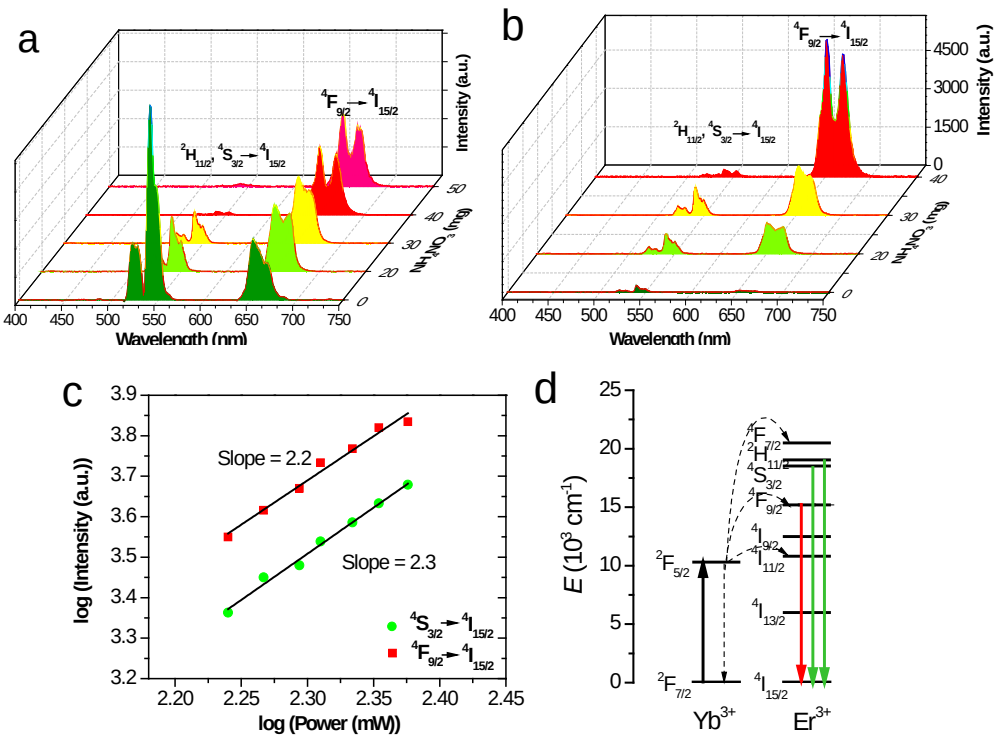

Fig. 2 Upconversion spectra of $NaGdF_4$:Yb, Er UCNPs prepared with various amounts of NH_4NO_3 per 2 mmol, normalized to Er^{3+} 655 nm emission (a) and actual emission (b). All of the UCNPs were excited at 980 nm with a 100 mW diode laser. (c) Power dependence of the green and red upconversion intensities (log-log) of $NaGdF_4$:Yb,Er UCNPs prepared with 20 mg of NH_4NO_3. (d) The energy level diagrams of the Er^{3+} and Yb^{3+} dopant ions and upconversion mechanisms under excitation of 980 nm. The full, dotted, and curly arrows represent emission, energy transfer and multiphonon-relaxation processes, respectively.

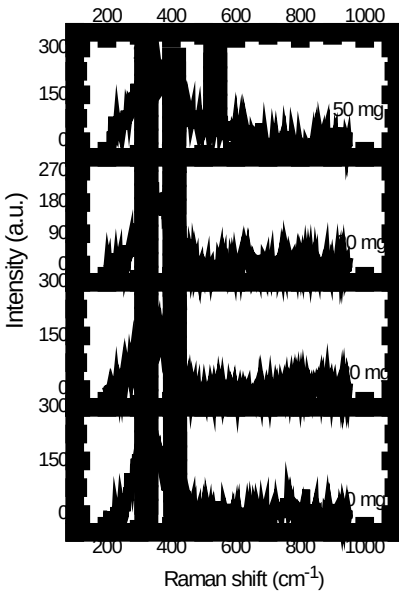

Fig. 3 Raman spectra of $NaGdF_4$ nanoparticles prepared with various amount of NH_4NO_3, 2 mmol. Due to the strong luminescence of Er^{3+} ion under ultra-violet laser excitation, the ratio of signal-to-noise of Raman spectra could be declined. Thus, the corresponding Yb and Er undoped $NaGdF_4$ nanoparticles were synthesized in the same way for the test of phonon energy by Raman spectroscopy.

relaxation from $^2H_{11/2}$, $^4S_{3/2}$ to $^4F_{9/2}$ and $^4I_{11/2}$ to $^4I_{13/2}$ levels determine the relative intensities of green to red emissions and color output of Er^{3+} ion (Fig. 2d).[22]

Lanthanide ion can be affected by the surrounding crystal field environment after doping into the host lattice according to thecrystal field theory. The phonon energy of host lattice (or host lattice vibration) could affect the multiphonon-nonradiative relaxation of the excited lanthanide ion. The nonradiative relaxation of excited 4f electron from a high-energy emitting level to a low-energy one can increase the populations of a low-energy emitting level, and thus enhance the light output in that level. According to Miyakawa-Dexter theory,[23] the multiphonon-nonradiative relaxation probability among various excited levels of lanthanide ion is expressed the following:

$$W_n(T) = W_0(0)[1-\exp(-h\nu / kT)]^{-n}$$

where $W_n(T)$ is the rate at temperature T, $W_0(0)$ is the rate at 0 K, $n = \Delta E/h\nu$, ΔE is the energy gap to the next level, and $h\nu$ is the phonon energy involved. The equation indicates the higher the phonon energy, the higher the nonradiative relaxation probability of excited lanthanide ion. The phonon energy of upconversion nanoparticles with different O^{2-} content were measured by Raman spectroscopy (Fig. 3). It is revealed that $NaGdF_4$ nanoparticles prepared with 0, 20, 30, and 50 mg of NH_4NO_3 exhibit the peak **1** positions at 323, 328, 332 and 335 cm^{-1}, respectively. The results show the red shift with increasing oxygen content. In addition, the relative intensities of peaks **2** (410 cm^{-1}) and **3** (538 cm^{-1}) increase gradually. These results indicated that the weighted average phonon energies of $NaGdF_4$:Yb, Er enhanced gradually with the increase of oxygen contents. This in turn has increased the multiphonon-nonradiative relaxation probabilities of excited Er^{3+} ion from $^2H_{11/2}$, $^4S_{3/2}$ to $^4F_{9/2}$ level and $^4I_{11/2}$ to $^4I_{13/2}$ level, and reduced the intensities ratio of green to red emissions, and therefore resulted in multicolor emission.[24]

It is noted that doping of O^{2-} ions not only facilitates the output of red emission but also greatly enhances the intensity of upconversion emission (Fig. 2b). The introduction of sufficient O^{2-} ions into $NaGdF_4$:Yb,Er led to a strong and enhanced red emission (Fig. 2b) due to the increase of particles size,[25] the multiphonon-nonradiative relaxation process and the change of crystal field symmetry of light-emitting lanthanide-ion. The increase of nanoparticle size enhanced the uponversion emission by reducing the surface quenching.[25] And the O^{2-} doping resulted multiphonon-nonradiative relaxation process can assist the transfer of energy originally belonging to the green-emitting levels to the red-emitting ones, and then also enhance the red emission (Fig. 2d). Furthermore, the doping O^{2-} ions dopant decreases the crystal field symmetry, which increases the transition probability of forbidden-transitional 4f electrons of lanthanide ions, thus further enhancing emission.[13b,13e] This phenomena are in consistent to the recent reports on Mn^{2+} ions doped nanoparticles.[13e,26] It is also observed the great splitting of red-emitting level of Er^{3+} ion when O^{2-} dopant content was higher than 7.13 wt%, indicating the decrease of crystal field symmetry of fcc $NaGdF_4$, further suggesting the doping of O^{2-} ions into $NaGdF_4$ crystal.[13e,27]

Oxygen ions doping mechanism

To elucidate the doping mechanism of O^{2-} ions, we added NH_4NO_3 into reaction solution at different temperatures and investigated the effect of that on the upconversion luminescent properties. It is observed that the relative intensities of red emission ($^4F_{9/2}\rightarrow{}^4I_{15/2}$ transition) of Er^{3+} ions increased with increasing the addition temperature from 120 to 250 ^oC (Fig.S2). When NH_4NO_3 was added into reaction solution at 300 ^oC, the relative intensity of red emission decreased again. Usually, the thermal decomposition mechanism of NH_4NO_3 was as follows lower than 150 ^oC:[17]

$$NH_4NO_3 \rightarrow HNO_3 + NH_3$$
$$4HNO_3 \rightarrow 4NO_2 + 2H_2O + O_2$$
$$NH_4NO_3 + 2NO_2 \rightarrow N_2 + H_2O + 2HNO_3$$

When the temperature was higher than 230 ^oC, NH_4NO_3 was decomposed as follows:

$$2NH_4NO_3 \rightarrow 2N_2 + O_2 + 4H_2O$$

Generally, oxygen atoms were first formed after decomposition of NH_4NO_3. Two formed oxygen atoms combined to form O_2. The formed oxygen atoms can be partially reduced to oxygen ions in the presence of octadecylamine molecule due to the reduction capability of amine group.[28] It is observed that more oxygen atoms were formed for a certain amount of NH_4NO_3

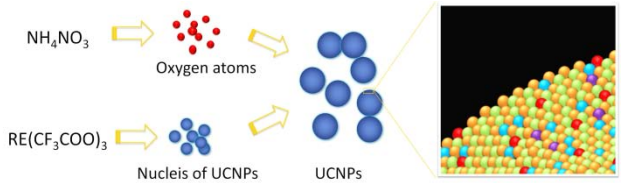

Scheme 2 Schematic illustration of O^{2-} ions doping mechanism.

when the temperature was higher than 230 °C. Correspondingly, more oxygen dopant would diffuse into the host lattice of fluoride nanoparticles, which facilitates the improvement of O^{2-} doping level in fluoride UCNPs and the enhancement of phonon energy, resulting in the increase of red emission. In addition, UCNPs were in large size when the temperature rises to 300 °C, because fluoride UCNPs began to nucleate and grow after decomposition of metal trifluoroacetate precursors at around 250 °C.[16,25] Although NH_4NO_3 can effectively decompose into oxygen atoms at 300 °C, it is difficult to further diffuse formed O^{2-} ions into host lattice of fluoride UCNPs with large size (See Supporting Information Fig. S6). Together, NH_4NO_3 was added into reaction system at the beginning stage of nucleation and growth process of fluoride UCNPs (at around 250 °C) facilitated the formation of enough oxygen atoms and the diffusion of that into fluoride host lattice (Scheme 2). Therefore, the improvement of red emission of Er^{3+} ions and the manipulation of the color output of fluoride UCNPs were easily achieved by adjusting the amount of NH_4NO_3.

Multicolor output of other fluoride UCNPs

To extend the generality of the control of oxygen doping in fluoride nanomaterials for color tuning and upconversion enhancement, we also synthesized $NaYF_4$:Yb, Er and $NaLuF_4$:Yb, Er UCNPs based on the above method. Similarly, we can also achieve the multicolor output of Yb/Er in other fluoride host lattices in the same way (Fig. 4). The red emission ($^4F_{9/2}\rightarrow{}^4I_{15/2}$) of Er^{3+} ions increased strongly with the increase the addition amounts of NH_4NO_3 (Fig. 4, S7 and S8). The relative intensities of green emission bands decreased rapidly. We can observe that the green emissions almost disappeared and only red emissions were exhibited for $NaYF_4$:Yb, Er and $NaLuF_4$:Yb, Er UCNPs after addition of 20 and 16 mg of NH_4NO_3, respectively. Correspondingly, the yellow-green, yellow, orange and red were shown. And upconversion emission intensities were also enhanced greatly. These results indicate that the multicolor tuning and upconversion enhancement of Er ion in other fluoride host lattices (*e.g.* $NaYF_4$ and $NaLuF_4$) can also be achieved based on controlling oxygen doping by adjusting the amount of NH_4NO_3. The present method may also be used for the rational control of O^{2-} doping level in other functional nanomaterials.

Application of multicolored UCNPs as color converter materials for LED devices

In a proof-of-concept, the oxygen doped fluoride UCNPs with multicolor emission and high photostability were used as color converter material in light emitting devices. The multicolored $NaGdF_4$:Yb, Er UCNPs were mixed with methyl methacrylate-butyl acrylate copolymer (P(MMA-co-BA)) to prepare nanocomposites. The nanocomposite with various amount of $NaGdF_4$:Yb, Er nanoparticles was fabricated and their upconversion spectra were measured. The upconversion intensities of nanocomposites were enhanced with the increasing of upconversion nanoparticles content (Fig. 5a). The color-converted LEDs exhibited bright near green, yellow-green, yellow and red output (Fig. 5b), which corresponded to the

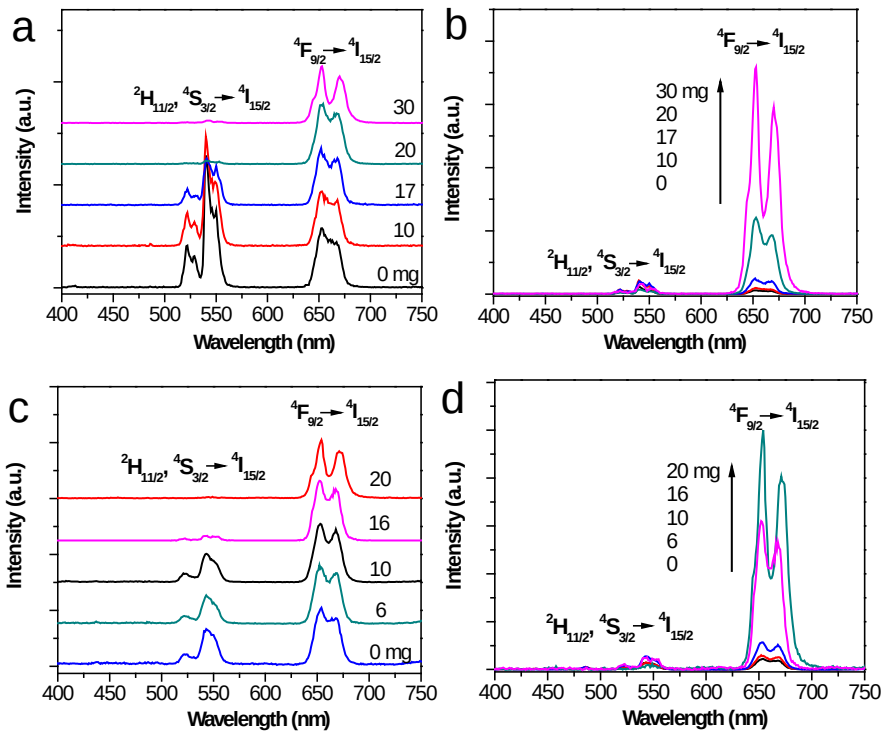

Fig. 4 Upconversion spectra of $NaYF_4$:Yb,Er (a) and $NaLuF_4$:Yb,Er (b) UCNPs prepared with various amount of NH_4NO_3 per 2 mmol (normalized to Er^{3+} 655 nm emission). All of the UCNPs were excited at 980 nm with a 260 mW diode laser.

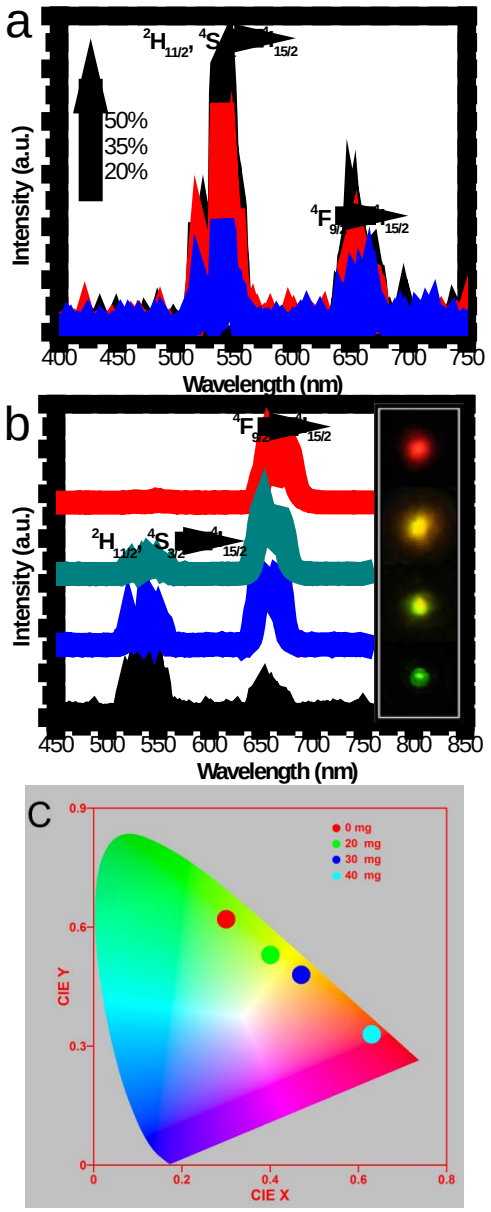

Fig. 5 (a) Upconversion emission spectra of $NaGdF_4$:Yb,Er polymer nanocomposite depending on the nanoparticles contents. (b) Upconversion emission spectra of different O^{2-} content $NaGdF_4$:Yb,Er polymer nanocomposites on NIR-LED devices. Inset: photos of the corresponding nanocomposites on the devices. (c) The corresponding CIE chromaticity coordinates of NIR-LED devices.

emission spectra of $NaGdF_4$:Yb, Er UCNPs with various oxygen content (Fig. 2). The corresponding Commission Internationale de l'Éclairage (CIE) coordinates were calculated and shown in Fig. 5c. If Yb/Tm codoped UCNPs with blue emission were incorporated, white LEDs could be obtained.[24d,29] In addition, we also characterized the magnetic properties of the as-prepared $NaGdF_4$:Yb, Er UCNPs to demonstrate the multifunctional properties. It is observed all the particles exhibit paramagnetism of around 1.5 emu/g at 20 KOe at room temperature (Fig. S9), which was close to the reported values of Gd-based nanoparticles.[2f,30] These multicolored fluoride UCNPs could be used not only for color-converting materials in full-color LED displays, but also for multiplexing bioassays and multi-modal imaging.[2f, 30]

Conclusions

In conclusion, we have successfully demonstrated a strategy to simultaneously manipulate multicolor output and enhance upconversion emission of Yb/Er doped fluoride UCNPs by controlling oxygen doping level. Ammonium nitrate was used as the oxygen source and added into reaction system at 250 °C to introduce the oxygen dopant. Multicolor tunability of $NaGdF_4$:Yb, Er UCNPs was realized by adjusting the phonon energy of host lattice by controlling oxygen doping level. Based on the O^{2-} ions doping effect, the prepared $NaGdF_4$:Yb, Er UCNPs further exhibited much enhanced upconversion luminescence and the splitting of red-emitting level. The tuning of upconversion behavior and upconversion enhancement of Er^{3+} ion in other fluoride host lattices was also realized in the same way. After incorporated into polymer, these multicolored UCNPs as color converter for light emitting devices were demonstrated. These multifunctional fluoride UCNPs with tuned multicolor are envisioned to be used in full-color LED displays, multiplexing bioassays and imaging (optical and magnetic resonance imaging). The present method for the rational control of O^{2-} doping level may also be used in other functional nanomaterials.

Acknowledgements

This work was supported by the National Natural Science Fundation of China (20836001, 21076038).

Notes and references

[a] *State Key Lab of Fine Chemicals, Dalian University of Technology, Dalian, 116024, China. Fax and Tel: 86 0411 84986265; E-mail: zhangshf@dlut.edu.cn*
b School of Materials Science and Engineering,Nanyang Technological University, 50 Nanyang Avenue, 639798, Singapore.

† Electronic Supplementary Information (ESI) available: upconversion spectra of $NaYF_4$:Yb, Er UCNPs prepared with various oxygen sources (trimethylamine *N*-oxide and ammonium carbonate, Fig. S1) and different addition temperatures of NH_4NO_3 (Fig. S2), enlarged XRD patterns (Fig. S3), the intensity ratios of green to red emissions of $NaGdF_4$:Yb,Er UCNPs prepared with various amounts of NH_4NO_3 (Fig. S4), power dependence of upconversion spectra of $NaGdF_4$:Yb,Er UCNPs prepared at 300 °C for 1h (Figure S5), upconversion spectra of the product after further reaction between as-prepared $NaYF_4$:Yb,Er and 50 mg of NH_4NO_3 at 300 °C for 1 h (Fig. S6), XRD patterns of $NaYF_4$:Yb, Er and $NaLuF_4$:Yb, Er UCNPs prepared with various amounts of NH_4NO_3 (Fig. S7 and S8), the corresponding magnetization curves of $NaGdF_4$:Yb, Er UCNPs (Fig. S9). See DOI: 10.1039/b000000x/.

1 a) D. W. Grainger, D. G. Castner, *Adv. Mater.* 2008, **20**, 867; b) R. Liu, D. Wu, S. Liu, K. Koynov, W. Knoll, Q. Li, *Angew. Chem. Int. Ed.* 2009, **121**, 4668.

2 a) F. Wang, D. Banerjee, Y. Liu, X. Chen and X. Liu, *Analyst* 2010, **135**, 1839; b) K. Kuningas, T. Ukonaho, H. Päkkilä, T. Rantanen, J. Rosenberg, T. Lövgren and T. Soukka, *Anal. Chem.* 2006, **78,** 4690; c) F. Wang, Y. Han, C. S. Lim, Y. Lu, J. Wang, J. Xu, H. Chen, C. Zhang, M. Hong and X. Liu, *Nature* 2010, **463**, 1061; d) G. Chen, T. Y. Ohulchanskyy, R. Kumar, H. Ågren and P. N. Prasad, *ACS NANO* 2010, **4**, 3163; e) M. Wang, C. C. Mi, W. X. Wang, C. H. Liu, Y. F. Wu, Z. R. Xu, C. B. Mao and S. K. Xu, *ACS NANO* 2009, **3**, 1580; f) P. Li, Q. Peng and Y. Li, *Adv. Mater.* 2009, **21**, 1945; g) C. Zhang, H. P. Zhou, L. Y. Liao, W. Feng, W. Sun, Z. X. Li, C. H. Xu, C. J. Fang, L. D. Sun and Y. W. Zhang, *Adv. Mater.* 2010, **22**, 633; h) J. H. Zeng, J. Su, Z. H. Li, R. X. Yan and Y. D. Li, *Adv. Mater.* 2005, **17**, 2119; i) G. B. Shan and G. P. Demopoulos, *Adv. Mater.* 2010, **22**, 4373; j) L. T. Su, S. K. Karuturi, J. Luo, L. Liu, X. Liu, J. Guo, T. C. Sum, R. Deng, H. J. Fan, X. Liu and A. I. Y. Tok, *Adv. Mater.* 2012, in press.

3 a) K. Douma, L. Prinzen, D. W. Slaaf, C. P. M. Reutelingsperger, E. A. L. Biessen, T. M. Hackeng, M. J. Post and M. A. M. J. Van Zandvoort, *Small* 2009, **5**, 544; b) N. Lewinski, V. Colvin and R. Drezek, *Small* 2008, **4**, 26; c) K. E. Sapsford, L. Berti and I. L. Medintz, *Angew. Chem. Int. Ed.* 2006, **45**, 4562; d) F. Wang and X. Liu, *Chem. Soc. Rev.* 2009, **38**, 976; e) X. Jia , J. Li and E. Wang *Nanoscale*, 2012, **4**, 5572; f) Q. Cheng , J. Sui and W. Cai, *Nanoscale*, 2012, **4**, 779.

4 a) R. Abdul Jalil and Y. Zhang, *Biomaterials* 2008, **29,** 4122; b) Z. Y. Hou, C. X. Li, P. A. Ma, Z. Y. Cheng, X. J. Li, X. Zhang, Y. L. Dai, D. M. Yang, H. Z. Lian and J. Lin, *Adv. Funct. Mater.* 2012, **22**, 2713; c) W. Wei, T. He, X. Teng, S. Wu, L. Ma, H. Zhang, J. Ma, Y. Yang, H. Chen, Y. Han, H. Sun and L. Huang, *Small*, 2012, **8**, 2271; d) J. Zhao, Z. Lu, Y. Yin, C. McRae, J. A. Piper, J. M. Dawes, D. Jin and E. M. Goldys, *Nanoscale*, 2013, **5**, 944; e) Y. Yang, F. Liu, X. Liu and B. Xing, *Nanoscale*, 2013, **5**,231; f) C. Li , J. Liu , S. Alonso, F. Li and Y. Zhang, *Nanoscale*, 2012, **4**, 6065.

5 a) S. Wu, G. Han, D. J. Milliron, S. Aloni, V. Altoe, D. V. Talapin, B. E. Cohen and P. J. Schuck, *Proceedings of the National Academy of Sciences* 2009, **106**, 10917; b) Y. I. Park, J. H. Kim, K. T. Lee, K. S. Jeon, H. B. Na, J. H. Yu, H. M. Kim, N. Lee, S. H. Choi and S. I. Baik, *Adv. Mater.* 2009, **21**, 4467.

6 a) C. L. Zhang, Y. X. Yuan, S. M. Zhang, Y. H. Wang and Z. H. Liu, *Angew. Chem. Int. Ed.* 2011, **50**, *6851*; b) J. L. Liu, Y. Liu, Q. Liu, C. Y. Li, L. N. Sun and F. Y. Li, *J. Am. Chem. Soc.* 2011, **133**, 15276.

7 B. Yan, J. C. *Boyer*, N. R. Branda and Y. Zhao, *J. Am. Chem. Soc.* 2011, **133**, 19714.

8 a) D. K. *Chatterjee*, A. J. Rufaihah and Y. Zhang, *Biomaterials* 2008, **29**, 937; b) L. Cheng, K. Yang, Y. G. Li, J. H. Chen, C. Wang, M. W. Shao, S. T. Lee and Z. Liu, *Angew. Chem. Int. Ed.* 2011, **50**, 7385.

9 a) N. M. Idris, Z. Li, L. Ye, E. K. Wei Sim, R. Mahendran, P. C. L. Ho and Y. Zhang, *Biomaterials* 2009, **30**, 5104; b) D. Vennerberg and Z. Lin, *Sci. Adv. Mater.*2011, **3**, 26; c) B. Dong, B. S. Cao, Y. Y. He, Z. Liu, Z. P. Li and Z. Q. Feng, *Adv. Mater.* 2012, **24**, 1987.

10 a) W. Niu, S. Wu, S. Zhang, J. Li and L. Li, *Dalton. Trans.* 2011, **40**, 3305; b) W. Niu, S. Wu, S. Zhang and L. Li, *Chem. Commun.*, 2010, **46**, 3908; c) W. Niu, S. Wu and S. Zhang, *J. Mater. Chem.*, 2011, **21**, 10894.

11 a) F. Wang, R. R. Deng, J. Wang, Q. X. Wang, Y. Han, H. M. Zhu, X. Y. Chen and X. G. Liu, *Nat. Mater.* 2011, **10**, 968; b) Q. Su, S. Han, X. Xie, H. Zhu, H. Chen, C.K. Chen, R.S. Liu, X. Chen, F. Wang and X. Liu, *J. Am. Chem. Soc.* 2012, **134**, 20849; c) Q. Zhang, X. Wang and Y. Zhu, *J. Mater. Chem.*2011, **21**, 12132.

12 a) Y. S. Liu, D. T. Tu, H. M. Zhu, R. F. Li, W. Q. Luo and X. Y. Chen, *Adv. Mater.* 2010, **22**, 3266; b) E. M. Chan, G. Han, J. D. Goldberg, D. J. Gargas, A. D. Ostrowski, P. J. Schuck, B. E. Cohen and D. J. Milliron, *Nano Lett.* 2012, **12**, 3839.

13 a) W. Niu, S. Wu and S. Zhang, *J. Mater. Chem.* 2010, **20**, 9113; b) J. Wang, F. Wang, C. Wang, Z. Liu and X. G. Liu, *Angew. Chem. Int. Ed.* 2011, **50**, 10369; c) F. Wang and X. Liu, *J. Am. Chem. Soc.* 2008, **130**, 5642; d) O. Ehlert, R. Thomann, M. Darbandi and T. Nann, *ACS NANO* 2008, **2**, 120; e) G. Tian, Z. J. Gu, L. J. Zhou, W. Y. Yin, X. X. Liu, L. Yan, S. Jin, W. L. Ren, G. M. Xing, S. J. Li and Y. L. Zhao, *Adv. Mater.* 2012, **24**, 1226.

14 a) Z. Li, Y. Zhang and S. Jiang, *Adv. Mater.* 2008, **20**, 4765-4769; b) H. X. Mai, Y. W. Zhang, L. D. Sun and C. H. Yan, *J. Phys. Chem. C* 2007, **111**, 13721.

15 D. Chen, Y. Yu, F. Huang, A. Yang and Y. Wang, *J. Mater. Chem.* 2011, **21**, 6186.

16 a) J. C. Boyer, F. Vetrone, L. A. Cuccia and J. A. Capobianco, *J. Am. Chem. Soc.* 2006, **128**, 7444; b) J. C. Boyer, L. A. Cuccia and J. A. Capobianco, *Nano Lett.* 2007, **7**, 847.

17 a) D. G. Patil, S. R. Jain and T. B. Brill, *Propellants, explosives, pyrotechnics* 1992, **17**, 99; b) R. Turcotte, P. Lightfoot, R. Fouchard and D. Jones, *J. Hazard. Mater.* 2003, **101**, 1.

18 Y. P. Du, Y. W. Zhang, L. D. Sun and C. H. Yan, *J. Phys. Chem. C* 2008, **112**, 405.

19 H. Liang, Y. Zheng, L. Wu, L. Liu, Z. Zhang and W. Cao, *J. Lumin.* 2012, **131**, 1802.

20 a) Z. Li and Y. Zhang, *Angew. Chem. Int. Ed.* 2006, **118**, 7896; b) C. Yan, A. Dadvand, F. Rosei and D. F. Perepichka, *J. Am. Chem. Soc.* 2010, **132**, 8868.

21 a) F. Vetrone, R. Naccache, V. Mahalingam, C. G. Morgan and J. A. Capobianco, *Adv. Funct. Mater.* 2009, **19**, 2924; b) F. Wang, J. A. Wang and X. G. Liu, *Angew. Chem. Int. Ed.* 2010, **49**, 7456.

22 a) J. Suyver, J. Grimm, K. Krämer and H. Güdel, *J. Lumin.* 2005, **114,** 53; b) N. J. J. Johnson, A. Korinek, C. H. Dong and F. C. J. M. van Veggel, *J. Am. Chem. Soc.* 2012, **134**, 11068.

23 a) T. Miyakawa and D. Dexter, *Phys. Rev. B* 1970, **1**, 70; b) T. Miyakawa and D. Dexter, *Phys. Rev. B* 1970, **1**, 2961.

24 a) Q. Lü, F. Y. Guo, L. Sun, A. Li and L. C. Zhao, *J. Phys. Chem. C* 2008, **112**, 2836; b) Y. Li, J. Zhang, X. Zhang, Y. Luo, X. Ren, H. Zhao, X. Wang, L. Sun and C. Yan, *J. Phys.Chem. C* 2009, **113**, 4413; c) W. Lu, X. Ma, H. Zhou, G. Chen, J. Li, Z. Zhu, Z. You and C. Tu, *J. Phys. Chem. C* 2008, **112**, 15071; d) G. Glaspell, J. Anderson, J. R. Wilkins and M. S. El-Shall, *J. Phys. Chem. C* 2008, **112**, 11527.

25 H. X. Mai, Y. W. Zhang, L. D. Sun and C. H. Yan, *J. Phys. Chem. C* 2007, **111**, 13730.

26 Y. Zhang, J. D. Lin, V. Vijayaragavan, K. K. Bhakoo and T. T. Y. Tan, *Chem. Commun.* 2012, **48**, 10322.

27 F. Auzel, *Chem. Rev.* 2004, *104*, 139.

28 a) C. Shen, C. Hui, T. Yang, C. Xiao, J. Tian, L. Bao, S. Chen, H. Ding and H. Gao, *Chem. Mater.* 2008, **20,** 6939; b) N. R. Jana and X. G. Peng, *J. Am. Chem. Soc.* 2003, **125**, 14280; c) N. F. Zheng, J. Fan and G. D. Stucky, *J. Am. Chem. Soc.* 2006, **128**, 6550; d) J. T. Ren and R. D. Tilley, *Small* 2007, **3**, 1508.

29 V. Mahalingam, F. Mangiarini, F. Vetrone, V. Venkatramu, M. Bettinelli, A. Speghini and J. A. Capobianco, *J. Phys. Chem. C* 2008, **112**, 17745.

30 a) R. Kumar, M. Nyk, T. Y. Ohulchanskyy, C. A. Flask and P. N. Prasad, *Adv. Funct. Mater.* 2009, **19**, 853; b) H. H. Gorris, R. Ali, S. M. Saleh and O. S. Wolfbeis, *Adv. Mater.* 2011, **23,** 1652.